

Large-System Performance of Iterative Multiuser Decision-Feedback Detection

Michael L. Honig, *Fellow, IEEE*, and Rapeepat Ratasuk, *Member, IEEE*

Abstract—The large-system performance of iterative multiuser decision-feedback detectors (DFDs) is studied for synchronous coded direct-sequence code-division multiple access. Both successive and parallel demodulation of users are considered. The filters are optimized according to the minimum mean-squared error criteria, assuming perfect feedback. We first consider Viterbi decoding with hard decision feedback, and compute union bounds on the large-system error rate. We then consider maximum *a posteriori* (MAP) decoding with soft decision feedback, and evaluate the error rate semianalytically by assuming the log-likelihood ratios computed by the MAP decoder are Gaussian random variables. Performance is studied numerically as a function of noise level, spectral efficiency, and code rate. Results show that soft decision feedback gives substantial gains relative to hard decision feedback. At moderate spectral efficiencies (users divided by bandwidth expansion less than 0.9), the iterative DFDs with soft decision feedback based on *a posteriori* probabilities can achieve near-single-user performance at an E_b/N_0 close to the large-system capacity bound.

Index Terms—Code-division multiple access (CDMA), decision feedback, large-system analysis, multiuser detection.

I. INTRODUCTION

SOFT iterative interference cancellation with single-user maximum *a posteriori* (MAP) decoding can offer a dramatic performance improvement relative to linear multiuser receivers [1]–[3]. Related schemes in which the interference canceller is replaced by a multiuser decision-feedback detector (DFD) optimized according to the minimum mean-squared error (MMSE) criterion have been proposed in [4] and [5]. When used in the reverse link of a cellular system, these receivers can, in principle, suppress other-cell interference while cancelling intracell users. In addition, relatively low-complexity adaptive implementations are possible, which do not require side information about channels and user spreading codes [6].

In this paper, we examine the large-system performance of iterative DFDs with randomly assigned signatures and convolutional codes. Specifically, we examine the error rate of the iterative DFDs as the number of users K , and processing gain N

both tend to infinity with fixed ratio K/N . Large-system analysis has been applied to linear and optimal multiuser receivers in [7]–[11], and has been shown to predict accurately the performance of finite-size systems of interest. Large-system analyses of noniterative DFDs have been presented in [12] and [13].

We first consider maximum-likelihood (ML), or Viterbi decoding with hard decision feedback, and derive a union bound on the large-system error rate for iterative DFDs with both parallel and successive demodulation. We then consider symbol-by-symbol MAP decoding with soft decision feedback, as proposed in [1]–[3]. The large-system analysis depends on the distribution of the soft feedback computed from the MAP decoder outputs. It has been observed that the distribution of the log-likelihood ratios (LLRs) at the output of a MAP decoder for an additive white Gaussian noise (AWGN) channel can be accurately approximated as Gaussian [5], [14]. A semianalytical approach is therefore used, in which the mean and variance of the LLRs for a *single-user* system with a particular convolutional code are determined by simulation. These estimates can then be used to compute the large-system performance with different system parameters (i.e., background noise level and load). In all cases, a key assumption is that the feedback is independent across users. Strictly speaking, this is true only in the limit of an infinitely long block length, and when the feedback is based on extrinsic information. A comparison with simulation results shows, however, that the analysis gives accurate performance predictions for finite block lengths, and when the (soft) feedback is computed from *a posteriori* probabilities (APPs).

Related work is presented in [15], where density evolution is combined with large-system analysis to determine the fixed points of iterative interference-cancellation techniques. The Gaussian approximation used here is also used in that paper to evaluate the asymptotic multiuser efficiency of soft parallel interference-cancellation schemes. A prior analysis of iterative soft parallel interference cancellation has been presented in [1], where the variance of the soft decisions at the output of the MAP decoder, and the variance of the interference at the input to the MAP decoder are computed iteratively. The large-system analysis presented here uses more information, namely, the distribution of the soft decisions which are being fed back for cancellation, and applies to the more general class of MMSE multiuser DFDs.

Numerical results are presented, which illustrate how the large-system performance depends on background signal-to-noise ratio (SNR), spectral efficiency K/N , and code rate. In general, successive demodulation reduces the number of iterations required for convergence relative to parallel demodu-

Paper approved by X. Wang, the Editor for Wireless Spread Spectrum of the IEEE Communications Society. Manuscript received January 23, 2002; revised August 22, 2002 and January 12, 2003. This work was supported by the National Science Foundation under Grant CCR-0073686. This paper was presented in part at the 2000 International Symposium on Information Theory, Sorrento, Italy, and the 2001 Information Theory Workshop, Cairns, Australia.

M. L. Honig is with the Department of Electrical and Computer Engineering, Northwestern University, Evanston, IL 60208 USA (e-mail: mh@ece.northwestern.edu).

R. Ratasuk is with the Motorola, Arlington Heights, IL 60004 USA (e-mail: ratasuk@cig.mot.com).

Digital Object Identifier 10.1109/TCOMM.2003.815041

lation. At moderate spectral efficiencies (i.e., $K/N < 0.9$), the iterative receivers can achieve near-single-user performance at an E_b/N_0 close to the lower bound corresponding to the large-system capacity [9]. The receivers are still interference limited in the sense that in the absence of noise, the error rate tends to 1/2 for large loads (users divided by chips per symbol). The maximum achievable spectral efficiency is obtained by letting the code rate approach one, and is slightly greater than two with soft decision feedback, and is approximately 1.53 with hard decision feedback. In contrast, the optimal multiuser detector is not interference limited [9].

The system model is described in the next section. Section III presents the analysis with hard decision feedback, and associated numerical results are presented in Section IV. Soft decision feedback with MAP decoding is then analyzed in Section V, and numerical results, which illustrate the effect of code rate on performance, are presented in Section VI. Extensions to more realistic code-division multiple-access (CDMA) models are briefly discussed in Section VII.

II. SYSTEM MODEL AND RECEIVERS

For simplicity, we consider an ideal synchronous CDMA system with perfect power control. Each user's sequence of information symbols ($\{b_k(i)\}$ for user k) is the input to a convolutional coder, assumed to be the same for each user, and the coder outputs are randomly interleaved before transmission through the ideal synchronous direct-sequence (DS)-CDMA channel. The number of chips per coded bit is $N' = RN$ where R is the code rate and N is the processing gain (bandwidth expansion factor). The received vector of N' samples during symbol interval i is given by

$$\mathbf{r}(i) = \mathbf{P}\mathbf{d}(i) + \mathbf{n}(i) \quad (1)$$

where $\mathbf{P} = [\mathbf{p}_1, \dots, \mathbf{p}_K]$ is the $N' \times K$ matrix of signatures, K is the number of users, $\mathbf{d}(i)$ is the i th vector of interleaved coded symbols across users, and $\mathbf{n}(i)$ is the vector of Gaussian noise samples with covariance matrix $\sigma^2\mathbf{I}_{N'}$, where \mathbf{I}_M is the $M \times M$ identity matrix. The signatures are random with independent and identically distributed (i.i.d.) elements, and the received power is normalized to one for all users. We assume binary information and coded symbols so that the k th element of $\mathbf{d}(i)$, $d_k(i) \in \{\pm 1\}$. We refer to $K/N = RK/N'$ as the *spectral efficiency* in bits per chip, since it is the normalized information rate summed over all users.

The received vector $\mathbf{r}(i)$ is the input to the DFD, consisting of the $N' \times K$ feedforward matrix \mathbf{F} , and the $K \times K$ feedback matrix \mathbf{B} . The output of the DFD corresponding to user k at time i and iteration m is

$$y_k^{(m)}(i) = \mathbf{F}_k^\dagger \mathbf{r}(i) - \tilde{\mathbf{B}}_k^\dagger \tilde{\mathbf{d}}_k^{(m-1)}(i). \quad (2)$$

where \dagger denotes complex conjugate transpose, \mathbf{M}_k is the k th column of the matrix \mathbf{M} , \mathbf{F}_k and $\tilde{\mathbf{B}}_k$ are the feedforward and feedback filters, respectively, and $\tilde{\mathbf{d}}_k^{(m)}(i)$ is the input to the feedback filter, all corresponding to the m th iteration for user k . The symbol estimates $\tilde{\mathbf{d}}_k^{(m)}$ are computed from the decoder outputs. The feedback matrix \mathbf{B} contains the columns $\{\tilde{\mathbf{B}}_k\}$ padded with zeros, as will be explained.

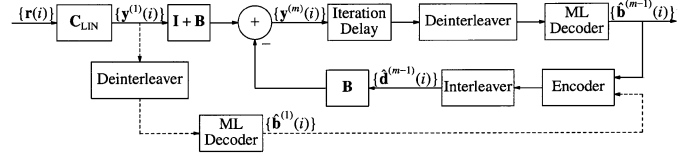


Fig. 1. Iterative receiver with ML decoding and hard parallel decision feedback.

The DFD filters are optimized according to the MMSE criterion with perfect feedback. This is in contrast to the MMSE and adaptive receivers proposed in [4]–[6] where the filters depend on the soft decoder outputs. A large-system analysis of those receivers appears to be quite difficult. Furthermore, numerical comparisons (for $K/N = 3/4$) indicate that although an adaptive DFD performs significantly better than the fixed-coefficient DFD for small systems [6], the performance gap diminishes as the system size increases.

Our objective is to select \mathbf{F}_k and $\tilde{\mathbf{B}}_k$ to minimize

$$\mathcal{E}_k = E \left[\left| d_k(i) - y_k^{(m)}(i) \right|^2 \right]. \quad (3)$$

In what follows, we will sometimes omit the dependence on iteration m and symbol i for convenience. We refer to the set of uncanceled users as U_k , and the set of cancelled users as \bar{U}_k . For the successive (S)-DFD, $U_k = \{k, \dots, K\}$ and $\bar{U}_k = \{1, \dots, k-1\}$, and for the parallel (P)-DFD, $U_k = \{k\}$ and $\bar{U}_k = \{1, \dots, k-1, k+1, \dots, K\}$. The vector $\tilde{\mathbf{d}}_k^{(m)}(i)$ in (2) has dimension $|\bar{U}_k|$. Furthermore, $\tilde{\mathbf{B}}_{\bar{U}_k} = \tilde{\mathbf{B}}_k$, where $\tilde{\mathbf{B}}_{\bar{U}_k}$ is the vector of elements in $\tilde{\mathbf{B}}_k$ with indexes in \bar{U}_k , and $\tilde{\mathbf{B}}_{U_k}$ contains only zeros.

With perfect feedback, i.e., $\tilde{\mathbf{d}} = \mathbf{d}$, the optimal \mathbf{F}_k and $\tilde{\mathbf{B}}_k$ are given by [16], [17]

$$\mathbf{F}_k = \mathbf{R}_{U_k}^{-1} \mathbf{p}_k \quad \tilde{\mathbf{B}}_k = \mathbf{P}_{\bar{U}_k}^\dagger \mathbf{F}_k \quad (4)$$

where the columns of the matrix \mathbf{P}_{U_k} are the signatures of the users in U_k , and

$$\mathbf{R}_{U_k} = \mathbf{P}_{U_k} \mathbf{P}_{U_k}^\dagger + \sigma^2 \mathbf{I}_{N'} \quad (5)$$

is the covariance matrix for the uncanceled users. That is, the feedforward filter is simply the linear MMSE receiver for the uncanceled users, and the backward filter is selected to cancel the interference from the remaining users. For the single-cell case considered, it is straightforward to show that the MMSE P-DFD reduces to the conventional (scaled) interference canceller, i.e., $\mathbf{F}_k = (1/(1 + \sigma^2))\mathbf{p}_k$ and $\tilde{\mathbf{B}}_k = (1/(1 + \sigma^2))(\mathbf{P}_{\bar{U}_k})^\dagger \mathbf{p}_k$. That is, the feedforward filter is a bank of matched filters.

III. HARD DECISION FEEDBACK

A block diagram of the iterative parallel (IP)-DFD receiver with hard decision feedback is shown in Fig. 1. Here, we represent the feedforward filter as $\mathbf{F} = \mathbf{C}_{\text{LIN}}(\mathbf{I} + \mathbf{B})$, where \mathbf{C}_{LIN} is the linear MMSE filter, and $\mathbf{I} + \mathbf{B}$ can be interpreted as an error-estimation filter [16], [17]. Specifically, $\mathbf{C}_{\text{LIN}} = \mathbf{R}^{-1}\mathbf{P}$ where $\mathbf{R} = \mathbf{P}\mathbf{P}^\dagger + \sigma^2\mathbf{I}_{N'}$, which gives the sequence of outputs $\{\mathbf{y}^{(1)}(i) = \mathbf{C}_{\text{LIN}}^\dagger \mathbf{r}(i)\}$ and the error

sequence $\{\mathbf{e}_{\text{LIN}}(i) = \mathbf{d}(i) - \mathbf{y}^{(1)}(i)\}$. The feedback filter \mathbf{B} is selected to minimize $E\{||(\mathbf{I} + \mathbf{B})^\dagger \mathbf{e}_{\text{LIN}}||^2\}$, where $\mathbf{B}_{k,m} = 0$ if $m \in U_k$. This representation is equivalent to the preceding expression (4), and appears in Fig. 1 since the linear MMSE filter is used for the first iteration. That is, the sequence $\{\mathbf{y}^{(1)}(i)\}$ is deinterleaved and decoded via the Viterbi algorithm, which gives a sequence of hard decisions $\{\hat{\mathbf{b}}^{(1)}(i)\}$. These are reencoded and interleaved to produce the sequence of estimated coded symbols $\{\hat{\mathbf{d}}^{(1)}\}$, which are used for feedback cancellation. The sequence of inputs $\{\mathbf{r}(i)\}$ and symbol estimates $\{\hat{\mathbf{d}}^{(1)}\}$ are then filtered according to (2) with $\hat{\mathbf{d}} = \hat{\mathbf{d}}^{(1)}$ to produce the sequence $\{\mathbf{y}^{(2)}(i)\}$, which is deinterleaved and input to the ML decoder. This process is then iterated.

For the IP-DFD, the vector $\hat{\mathbf{d}}_k^{(m-1)}$ does not depend on k , i.e., decisions from the preceding iteration are used for parallel cancellation. For the iterative successive (IS)-DFD, the most recent decisions are used for cancellation. That is, for the first iteration, the S-DFD is used, in which users are successively demodulated and cancelled. The filters for user k are given by (4). In succeeding iterations, the users are reordered, and the feedback filter \mathbf{B}_k cancels *all* demodulated users. That is, the filters are P-DFD filters, but the users are successively demodulated. For the IS-DFD, the decision vector, which is fed back for cancellation, is denoted as $\hat{\mathbf{d}}_k^{(m)}$, where the first $k-1$ elements (with the new ordering) are from the current iteration, and the remaining decisions are from the preceding iteration.

In what follows, we will assume that the error events are independent across users. This is true provided the following two conditions are satisfied: 1) the block length tends to infinity, and each user has a random interleaver, which is independent of the interleavers for the other users; 2) the symbol estimate, which is fed back for cancellation, does not depend on the current input $\mathbf{r}(i)$. In the case of the ML decoder, the second condition requires that the contribution from the current input be subtracted from the decision metrics. Even without this modification, numerical examples, which follow, indicate that the error independence assumption leads to analytical results, which accurately predict performance in the region of interest.

A. IP-DFD

For the IP-DFD, we have

$$y_k^{(m)}(i) = \eta \left[d_k(i) + \psi_{\mathcal{E}}^{(m)} + \mathbf{p}_k^\dagger \mathbf{n}(i) \right] \quad (6)$$

where the elements of \mathbf{p}_k are i.i.d. random variables, $E[||\mathbf{p}_k||^2] = 1$, η is a constant, and

$$\psi_{\mathcal{E}}^{(m)} = \sum_{l \neq k} \left(\mathbf{p}_k^\dagger \mathbf{p}_l \right) \left[d_l(i) - \hat{d}_l^{(m-1)}(i) \right] \quad (7)$$

is the feedback error term. Let $\bar{K} = K/N'$ denote the normalized load. Assuming that the error events are independent across users, as $K \rightarrow \infty$ with fixed \bar{K} , the feedback error term becomes Gaussian with mean zero and variance given by

$$E \left[\left| \psi_{\mathcal{E}}^{(m)} \right|^2 \right] = 4P^{(m-1)} \bar{K} \quad (8)$$

where $P^{(m)} = \text{Pr}\{d_l \neq \hat{d}_l^{(m)}\}$ is the probability of error for the coded bits at iteration m .

The SINR at the input to the ML decoder at iteration m is, therefore

$$\beta_{\text{IP-DFD}}^{(m)} = \frac{1}{4P^{(m-1)} \bar{K} + \sigma^2}. \quad (9)$$

The following analysis is consistent with the error independence assumption when $P^{(m-1)}$ is the error probability associated with an ML decoder, which uses only extrinsic information. Because the performance with a standard ML decoder is of primary interest, we will instead use the standard union bound to evaluate the coded error rate. Strictly speaking, the error independence assumption is no longer valid; however, comparisons with simulation results indicate that it still gives accurate performance predictions. Since the large-system interference plus noise is Gaussian, the union bound is given by

$$P^{(m)} = \sum_{l \geq d_{\text{free}}} w_l \mathcal{P} \left(\beta_{\text{IP-DFD}}^{(m)}; l \right) \quad (10)$$

where w_l is the number of information bits corresponding to error paths of weight l , d_{free} is the minimum free distance of the code, and $\mathcal{P}(\beta; l)$ is the pairwise error probability for a path of weight l at SNR β .

For the first iteration, the large-system error rate is computed for the linear MMSE receiver by computing the corresponding large-system output SINR [8]

$$\beta_{\text{LIN}} = \lim_{K \rightarrow \infty} \mathbf{p}_k^\dagger \mathbf{R}_{k-}^{-1} \mathbf{p}_k = \frac{1}{\sigma^2 + \frac{\bar{K}}{1 + \beta_{\text{LIN}}}} \quad (11)$$

which is independent of user, where $\mathbf{R}_{k-} = \mathbf{R} - \mathbf{p}_k \mathbf{p}_k^\dagger$ is the interference-plus-noise covariance matrix for user k . The output interference plus noise becomes Gaussian as $K \rightarrow \infty$ [18], so that the error rate for the coded bits can again be bounded according to (10), where $\beta_{\text{IP-DFD}}$ is replaced by β_{LIN} .

The procedure for computing the large-system error rate for the IP-DFD follows.

- 1) For $m = 1$, compute the large-system output SINR for the linear MMSE receiver from (11).
- 2) Compute the union bound on coded bit-error probability from (10). Alternatively, this can be obtained by simulating a single-user system.
- 3) Compute the SINR at the output of the P-DFD from (9).
- 4) Iterate steps 2 and 3. Compute the bit-error probability at the final iteration from the corresponding union bound, or by simulation.

B. IS-DFD

The analysis for the IS-DFD is more complicated than that for the IP-DFD, since the performance of a particular user depends on the ordering. To equalize the performance over the user population, we reverse the order of the users from iteration to iteration. For the first iteration, the S-DFD is used, which has output

$$y_k(i) = \kappa_k d_k(i) + \psi_{I;k} + \psi_{\mathcal{E};k}^{(1)} + \mathbf{p}_k^\dagger \mathbf{R}_{U_k}^{-1} \mathbf{n}(i) \quad (12)$$

where $\kappa_k = \mathbf{p}_k^\dagger \mathbf{R}_{U_k}^{-1} \mathbf{p}_k$

$$\psi_{I;k} = \sum_{j \in U_k} \left(\mathbf{p}_k^\dagger \mathbf{R}_{U_k}^{-1} \mathbf{p}_j \right) d_j(i) \quad (13)$$

is the interference from undetected users, and

$$\psi_{\mathcal{E};k}^{(1)} = \sum_{l \in \bar{U}_k} \left(\mathbf{p}_k^\dagger \mathbf{R}_U^{-1} \mathbf{p}_l \right) \left[d_l(i) - \hat{d}_l^{(1)}(i) \right] \quad (14)$$

is the feedback error term for iteration $m = 1$, all for user k . We define the normalized user index $\bar{k} = k/K$. As $K \rightarrow \infty$, the set of values, which \bar{k} can assume is dense in the interval $(0,1)$. With perfect cancellation, the ‘‘effective’’ load for user k is $(K - k + 1)/N'$, which has large-system limit $\bar{K}(1 - \bar{k})$. In what follows, we will always show the large-system user index \bar{k} as a function argument.

Referring to (12), with random signatures, as $K \rightarrow \infty$, κ_k converges in probability to a constant [8], and $\psi_{I;k}$ becomes a zero-mean Gaussian random variable [18]. Assuming d_l and $\hat{d}_l^{(1)}$ are independent of d_n and $\hat{d}_n^{(1)}$ for $l \neq n$, which is reasonable for sufficiently large interleaving depths, $\psi_{\mathcal{E};k}^{(1)}$ also becomes zero-mean Gaussian. We can then evaluate the large-system error rate by evaluating the large-system limit of the output SINR

$$\beta_{\text{S-DFD}}(\bar{k}) = \lim_{K \rightarrow \infty} \frac{\kappa_k^2}{E\left(|\psi_{I;k}|^2\right) + E\left(|\psi_{\mathcal{E};k}^{(1)}|^2\right) + \sigma^2 \gamma_k} \quad (15)$$

where $\gamma_k = \mathbf{p}_k^\dagger \mathbf{R}_{U_k}^{-2} \mathbf{p}_k$, and the expectations are over the data symbols only.

As $K \rightarrow \infty$, we show in the Appendix that

$$\kappa_k \rightarrow \kappa^*(\bar{k}) = \frac{\beta_{\text{LIN}}(\bar{k})}{1 + \beta_{\text{LIN}}(\bar{k})} \quad (16)$$

$$\begin{aligned} \gamma_k \rightarrow \gamma^*(\bar{k}) &= \frac{1}{1 + \beta_{\text{LIN}}(\bar{k})} \\ &\times \frac{\beta_{\text{LIN}}(\bar{k})}{\sigma^2 [1 + 2\beta_{\text{LIN}}(\bar{k})] + \bar{K}(1 - \bar{k}) - 1} \end{aligned} \quad (17)$$

$$E\left(|\psi_{I;k}|^2\right) \rightarrow \psi^*(\bar{k}) = \frac{\beta_{\text{LIN}}(\bar{k})}{[1 + \beta_{\text{LIN}}(\bar{k})]^2 - \sigma^2 \gamma^*(\bar{k})} \quad (18)$$

where convergence is in probability. We emphasize that the function argument \bar{k} denotes user index, and the corresponding load is $\bar{K}(1 - \bar{k})$.

To evaluate the variance of the feedback error term (14), we again assume that d_l and $\hat{d}_l^{(1)}$ are each independent of d_n and $\hat{d}_n^{(1)}$ for $l \neq n$, so that

$$E\left(|\psi_{\mathcal{E};k}^{(1)}|^2\right) = 4 \sum_{l \in \bar{U}_k} P_l^{(1)} E\left(\left|\mathbf{p}_k^\dagger \mathbf{R}_{U_k}^{-1} \mathbf{p}_l\right|^2\right) \quad (19)$$

$$= \frac{4}{N'} \sum_{l \in \bar{U}_k} P_l^{(1)} E\left(\mathbf{p}_k^\dagger \mathbf{R}_{U_k}^{-2} \mathbf{p}_k\right) \quad (20)$$

$$= 4\bar{K} E\left(\mathbf{p}_k^\dagger \mathbf{R}_{U_k}^{-2} \mathbf{p}_k\right) \left(\frac{1}{K} \sum_{l \in \bar{U}_k} P_l^{(1)}\right) \quad (21)$$

where the expectation is with respect to both the random signatures and the data symbols, $P_l^{(1)} = \Pr\{d_l \neq \hat{d}_l^{(1)}\}$, and we have used the fact that \mathbf{p}_l is independent of \mathbf{R}_{U_k} and \mathbf{p}_k . As $K \rightarrow \infty$, we have

$$E\left(|\psi_{\mathcal{E};k}^{(1)}|^2\right) \rightarrow \xi^{(1)}(\bar{k}) = 4\bar{K} \gamma^*(\bar{k}) \int_0^{\bar{k}} P^{(1)}(x) dx \quad (22)$$

where $\gamma^*(\bar{k})$ is given by (17), and $P^{(1)}(x)$ for $x \in (0,1)$ is the limit of the sequence $\{P_1^{(1)}, \dots, P_K^{(1)}\}$ as $K \rightarrow \infty$, where $l/K \rightarrow x$.

The large-system error rate for the S-DFD can be evaluated numerically by integrating (15) and (22) across users. Specifically, let $G(\beta)$ denote the large-system error probability for the coded bits at the output of the ML decoder as a function of input SNR β , assuming a single-user AWGN channel. Then

$$P^{(1)}(\bar{k}) = G\left[\beta_{\text{S-DFD}}(\bar{k})\right] \quad (23)$$

where

$$\beta_{\text{S-DFD}}(\bar{k}) = \frac{[\kappa^*(\bar{k})]^2}{\psi^*(\bar{k}) + \xi^{(1)}(\bar{k} - \Delta) + \sigma^2 \gamma^*(\bar{k})} \quad (24)$$

is the large-system output SINR of the S-DFD for user \bar{k} , and can be computed from (16)–(18) and (22), and Δ is the integration step size. The new value $P^{(1)}(\bar{k})$ is then used to compute $\xi^{(1)}(\bar{k})$ from (22), which is used in (24) to compute $\beta_{\text{S-DFD}}(\bar{k} + \Delta)$, and so forth. The boundary condition is $P^{(1)}(0) = G[\beta_{\text{LIN}}(0)]$, where $\beta_{\text{LIN}}(0)$ is the SINR for the linear MMSE receiver with load \bar{K} , which corresponds to $\bar{k} = 0$.

In the large-system limit, the error rate for the S-DFD decreases monotonically with user index, provided that the initial SINR for user index $\bar{k} = 0$ is sufficiently high. In subsequent iterations $m > 1$, the S-DFD is replaced by the IS-DFD, where the order of the users is reversed at each iteration. The corresponding feedback error term for a finite system is

$$\psi_{\mathcal{E};k}^{(m)} = \sum_{l \neq k} \left(\mathbf{p}_k^\dagger \mathbf{p}_l \right) \left[d_l^{(m)}(i) - \hat{d}_l^{(m)}(i) \right] \quad (25)$$

and depends on k . As $K \rightarrow \infty$

$$\begin{aligned} E\left(|\psi_{\mathcal{E};k}^{(m)}|^2\right) &\rightarrow \xi^{(m)}(\bar{k}) = 4\bar{K} \\ &\times \left(\int_0^{\bar{k}} P^{(m)}(x) dx + \int_{\bar{k}}^1 P^{(m-1)}(x) dx \right) \end{aligned} \quad (26)$$

The two integrals on the right represent the contribution of users $l < k$ and $l > k$ to the feedback error variance, respectively, assuming the new ordering. The output SINR for user \bar{k} is

$$\beta_{\text{IS-DFD}}^{(m)}(\bar{k}) = \frac{1}{\xi^{(m)}(\bar{k}) + \sigma^2} \quad (27)$$

and the procedure for computing the error rates across users is the same as for the S-DFD where the SINR is given by (27), and the feedback error variance is given by (26). Of course, numerical computation of the error rate requires that the integrals in (22) and (26) be approximated as sums.

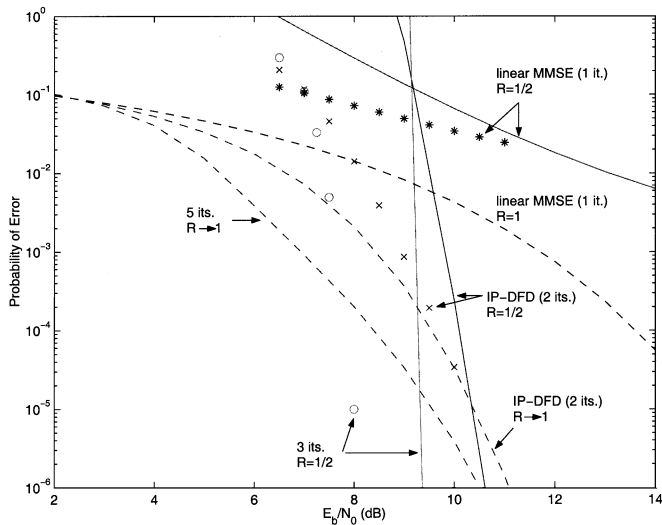


Fig. 2. Large-system error rate for the IP-DFD with hard decision feedback. Discrete points are from simulation with $K = 120$: “*”, “x”, and “o” correspond to the linear, P-DFD, and IP-DFD with two iterations, respectively, with $R = 1/2$.

TABLE I
CONVOLUTIONAL CODES FROM [19] USED TO GENERATE NUMERICAL RESULTS. ACG IS ASYMPTOTIC CODING GAIN. THE RATE 7/8 CODE IS A PUNCTURED RATE 1/8 CODE WITH 256 STATES

R	# states	d_{free}	ACG [dB]
1/4	64	20	7.0
1/2	64	10	7.0
3/4	64	6	6.5
7/8	256	4	5.4

IV. NUMERICAL RESULTS: HARD DECISION FEEDBACK

In this section, we show large-system performance results for the IP-DFD with hard decision feedback. Additional numerical results show that the error rates for both the IP- and IS-DFDs converge to the same value with sufficient iterations. We defer a comparison of IP- and IS-DFD performance to Section VI-A, which presents results with soft decision feedback.

Fig. 2 shows plots of large-system bit-error rate (BER) versus E_b/N_0 for the IP-DFD with hard decision feedback with spectral efficiency $K/N = R\bar{K} = 0.75$ and code rate $R = 1/2$. Properties of the convolutional codes used to generate all numerical results are shown in Table I. Also shown are plots corresponding to $R \rightarrow 1$, and simulation results for the coded P-DFD with $K = 120$. The former plots assume that $R \rightarrow 1$ from below with perfect interleaving. With coding we note that only three iterations are needed for the error rate to converge. (The first two iterations correspond to the linear and noniterative P-DFD, respectively.) The rate 1/2 code improves performance only when E_b/N_0 is relatively high. This is because for the rate 1/2 code, there are $N/2$ chips per bit, and hence, fewer degrees of freedom are available for interference suppression than for $R \rightarrow 1$. The input SINR for the code must exceed a sufficient threshold before the benefit of the coding gain is realized.

Fig. 3 shows large-system error rate versus spectral efficiency K/N when the background noise is negligible. (We chose $E_b/N_0 = 100$ dB.) Curves for different convolutional code rates are shown, including $R \rightarrow 1$. The codes have

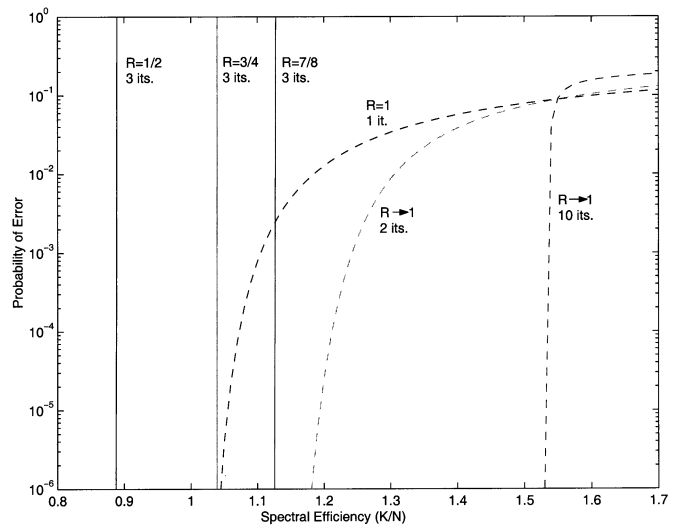


Fig. 3. Large-system error rate versus spectral efficiency K/N with hard decision feedback for very large E_b/N_0 .

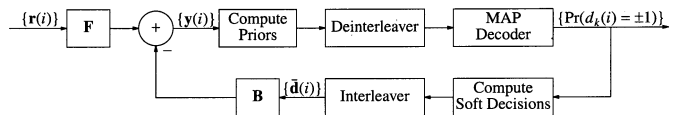


Fig. 4. Iterative receiver with MAP decoding and soft decision feedback.

been selected from [19] on the basis of similar constraint lengths and performance. (See Table I.) The vertical curve associated with each code is specified by a load threshold, below which the union bound does not converge. Above the threshold, the interference is perfectly cancelled, and since the noise is negligible, the error rate is essentially zero. The maximum spectral efficiency is achieved by letting $R \rightarrow 1$, and is approximately 1.52. We remark that with coding, the noniterative P-DFD achieves nearly the same performance as the IP-DFD, and the corresponding error-rate curves are nearly vertical. Approximately ten iterations are needed for the IP-DFD to converge with $R \rightarrow 1$.

V. SOFT DECISION FEEDBACK

We now refer to Fig. 4, in which a MAP decoder computes $q = \Pr[d_k(i) = 1]$ for each $k = 1, \dots, K$ and i . The soft estimate of d_k at iteration m , which is fed back for cancellation, is $\bar{d}_k^{(m)} = E[d_k] = 2q - 1$. For the IP-DFD, the i th input to the MAP decoder for user k is

$$y_k^{(m)}(i) = \eta \times \left[d_k(i) + \sum_{l \neq k} (\mathbf{p}_k^\dagger \mathbf{p}_l) [d_l(i) - \bar{d}_l^{(m-1)}(i)] + \mathbf{p}_k^\dagger \mathbf{n}(i) \right]. \quad (28)$$

In analogy with the error independence assumption for hard decision feedback, we will assume that the terms in the sum (feedback error terms) are independent across users. This assumption is valid provided that the users have independent random interleavers, and that each soft feedback estimate $\bar{d}_k^{(m)}$ is obtained from extrinsic information. Let $q_{\text{APP}}(i)$ denote the full APP computed by the MAP decoder for the i th symbol, and let

$q_{\text{EXT}}(i)$ denote the corresponding probability based on extrinsic information. Then the LLR $\log[q_{\text{EXT}}(i)/(1 - q_{\text{EXT}}(i))] = \log[q_{\text{APP}}(i)/(1 - q_{\text{APP}}(i))] - \log[g(i)/(1 - g(i))]$, where $g(i) = \text{Pr}[d_k(i) = 1|y_k^{(m)}(i)]$ is the APP computed from the *current* input. Strictly speaking, the error independence assumption is not true when APPs are used to compute the soft feedback. However, a comparison with simulation results shows that the following analysis accurately predicts performance (with APPs) over a wide region of interest.

Letting $K = \bar{K}N \rightarrow \infty$, the second term in the bracket (feedback error term) becomes Gaussian with mean zero and variance given by

$$\xi^{(m)} = \bar{K} \int (1-x)^2 dF_{\bar{d}_k^{(m-1)}|d_k=1}(x) \quad (29)$$

where $F_{\bar{d}_k^{(m)}|d_k=1}(x)$ is the distribution of $\bar{d}_k^{(m)}$ given that the coded symbol $d_k = 1$. Given $\xi^{(m)}$ and σ , the large-system decoded error rate is the same as that for a *single* user transmitting over an AWGN channel, where the SNR is $1/(\xi^{(m)} + \sigma^2)$. This error rate can be obtained by simulating the single-user system, or can be estimated via a union bound.

To obtain $F_{\bar{d}_k^{(m)}|d_k=1}(x)$, we use the approximation that the LLR $\log[q_1/(1 - q_1)]$, where q_1 is the random variable q computed by the MAP decoder conditioned on $d_k(i) = 1$, is a Gaussian random variable with mean μ_{LLR} and variance σ_{LLR}^2 [14], [20]. The corresponding density is given by

$$f_{\bar{d}_k^{(m)}|d_k=1}(x) = \sqrt{\frac{2}{\pi\sigma_{\text{LLR}}^2}} \frac{1}{1-x^2} \times \exp\left(-\frac{2 \tanh^{-1}(x) - \mu_{\text{LLR}}}{2\sigma_{\text{LLR}}^2}\right) \quad (30)$$

where \tanh^{-1} denotes inverse hyperbolic tangent. Examples corresponding to different iterations m at $E_b/N_0 = 4$ dB are shown in Fig. 5. The quantities μ_{LLR} and σ_{LLR}^2 , as a function of SNR, are obtained by simulating the equivalent single-user AWGN system.

The large-system error rate for the IP-DFD with soft feedback can be computed according to the following procedure.

- 1) For the first iteration, compute the large-system output SINR for the linear MMSE receiver from (11) along with the corresponding error rate.
- 2) Look up μ_{LLR} and σ_{LLR}^2 as a function of the SINR computed at the preceding step 1 or 3.
- 3) Compute the variance of the feedback error term $\xi^{(m)}$ from (29) and (30), which determines the SINR at the input to the MAP decoder.
- 4) Compute or look up the single-user decoded error rate.
- 5) Iterate steps 2, 3, and 4.

The analysis for the soft IS-DFD is analogous to that for the hard IS-DFD. Namely, for the first iteration the output SINR for the S-DFD is again given by (15) where κ_k , $E(|\psi_{I;k}|^2)$, and γ_k have the large-system limits in (16), (17), and (18), respectively. In this case

$$\psi_{\xi;k}^{(1)} = \sum_{l \in \bar{U}_k} \left(\mathbf{p}_k^\dagger \mathbf{R}_{U_k}^{-1} \mathbf{p}_l \right) \left[d_l(i) - \bar{d}_l^{(1)}(i) \right] \quad (31)$$

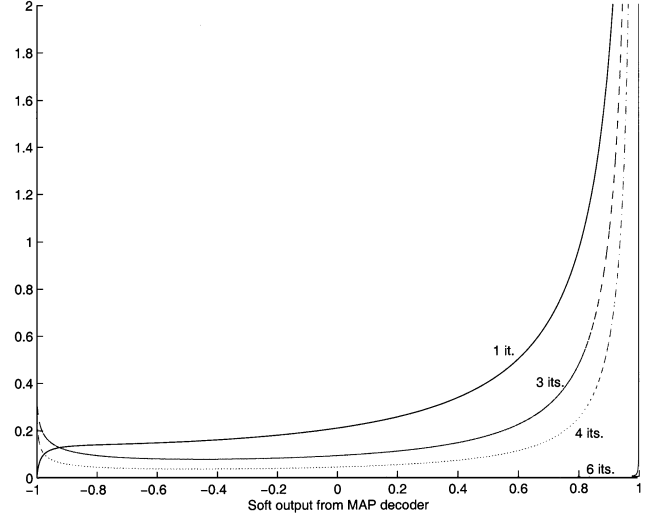


Fig. 5. Probability density functions (30) for different iterations at $E_b/N_0 = 4$ dB.

is the feedback error term, and again assuming that d_l and $\bar{d}_l^{(1)}$ are each independent of d_n and $\bar{d}_n^{(1)}$ for $l \neq n$, we have, in analogy with (21)

$$E\left(|\psi_{\xi;k}^{(1)}|^2\right) = \frac{1}{N'} \sum_{l \in \bar{U}_k} E\left(\mathbf{p}_k^\dagger \mathbf{R}_{U_k}^{-2} \mathbf{p}_k\right) \delta_l \quad (32)$$

where $\delta_l = E(|d_l - \bar{d}_l^{(1)}|^2 | d_l = 1)$ is given by (29) and (30), and the expectation is with respect to both the random signatures and the data symbols. As $K \rightarrow \infty$, we have

$$E\left(|\psi_{\xi;k}^{(1)}|^2\right) \rightarrow \xi^{(1)}(\bar{k}) = \bar{K} \gamma^*(\bar{k}) \int_0^{\bar{k}} \delta(x) dx \quad (33)$$

where $\gamma^*(\bar{k})$ is given by (17), and $\delta(x)$ for $x \in (0, 1)$ is the large-system limit of the sequence $\{\delta_1, \dots, \delta_K\}$, where $l/K \rightarrow x$.

The large-system error rate for the soft S-DFD is evaluated by numerically integrating (33) across users according to the following procedure, where Δ is the integration step-size.

- 1) For $\bar{k} = 0$, the output SINR, error rate, and corresponding values of μ_{LLR} , σ_{LLR} , and $\xi^{(1)}(0)$, are evaluated for the linear MMSE receiver.
- 2) The large-system SINR at the input to the MAP decoder for user $\bar{k} + \Delta$ is computed from (24), (16)–(18) and (33).
- 3) $\xi^{(1)}(\bar{k} + \Delta)$ is computed from (29) and (30) using values for μ_{LLR} and σ_{LLR} corresponding to the SINR from the preceding step.
- 4) The user index \bar{k} is replaced by $\bar{k} + \Delta$, and steps 2 and 3 are repeated.

In this way, the large-system output SINR and corresponding error rate can be evaluated for $\bar{k} = n\Delta$, $n = 0, 1, \dots, \Delta^{-1}$.

In succeeding iterations, the S-DFD is replaced by the IS-DFD, where the order of the users is reversed at each

iteration. The output SINR for user \bar{k} at iteration m is then given by (27) where the feedback error term

$$\psi_{\varepsilon,k}^{(m)} = \sum_{l \neq k} (\mathbf{p}_k^\dagger \mathbf{p}_l) \left[d_l^{(m)}(i) - \bar{d}_l^{(m)}(i) \right] \quad (34)$$

depends on k , and $\bar{d}_l^{(m)}$ contains estimates from both the current and preceding iterations. As $K \rightarrow \infty$

$$E \left(\left| \psi_{\varepsilon,k}^{(m)} \right|^2 \right) \rightarrow \xi^{(m)}(\bar{k}) = \bar{K} \left(\int_0^{\bar{k}} \delta^{(m)}(x) dx + \int_{\bar{k}}^1 \delta^{(m-1)}(x) dx \right) \quad (35)$$

where $\delta^{(m)}(x)$ is the variance of the feedback error term for user x at iteration m . The procedure for computing the error rates across users is then the same as for the S-DFD, where the SINR is given by (27), and the feedback error variance is given by (35).

VI. NUMERICAL RESULTS: SOFT DECISION FEEDBACK

A. Comparison of IP- and IS-DFDs

Fig. 6 shows plots of large-system BER versus E_b/N_0 for the IP-DFD with spectral efficiency $K/N = R\bar{K} = 0.75$ and code rate $R = 1/2$. Simulated points corresponding to $K = 120$ are also shown. The results in Fig. 6(a) and (b) assume soft feedback based on extrinsic information and APPs, respectively. The single-user coded error rate as a function of SNR was determined by simulation for error rates greater than 10^{-3} , and by computing the union bound for error rates less than 10^{-3} . For this example, the E_b/N_0 corresponding to the large-system capacity at a spectral efficiency of 0.75 bit/chip is approximately 3.2 dB. Comparisons with simulation results for smaller systems shows that the large system requires relatively few iterations to converge even at an E_b/N_0 close to the steep part of the curve.

Fig. 6 shows that the large-system results accurately predict the simulated results for the number of iterations shown. This is true for both extrinsic feedback and feedback based on APPs. For the case of APP feedback, increasing the number of iterations beyond five shifts the large-system “drop-off” point by approximately one dB to the left, whereas the simulated drop-off point does not change. This inaccuracy may be caused in part by the dependence among soft feedback decisions, as pointed out earlier. However, further investigation indicates that the main reason for this inaccuracy is that after a few iterations, the decoder decisions begin to harden, and introduce errors into the feedback filter, which are not accounted for in the large-system analysis. In other words, after a few iterations, the distribution for the LLRs at the output of the MAP decoder become skewed, thereby violating the Gaussian assumption. (This appears to be less of a problem with extrinsic feedback since only five iterations are needed for convergence.) We find, however, that at higher loads, the large-system analysis with APP feedback remains accurate for a larger number of iterations.

Comparing Fig. 6(a) and (b), we see that large-system performance with soft decision feedback based on APPs provides a substantial performance gain relative to extrinsic feedback. The degradation in performance due to biased interference estimates, associated with APPs [15], is therefore outweighed by

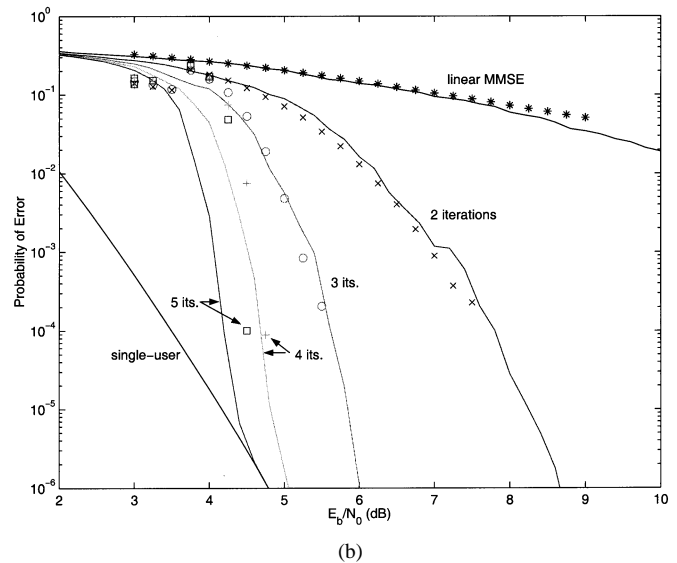
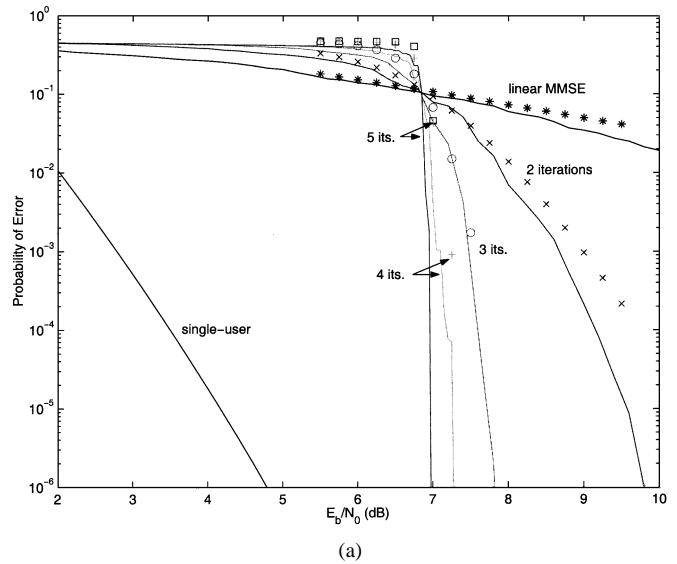


Fig. 6. Large-system error rate versus E_b/N_0 for the IP-DFD with soft feedback. Discrete points are from simulation with $K = 120$. The code rate $R = 1/2$ and the spectral efficiency $K/N = 3/4$. (a) The soft feedback symbols are computed from extrinsic information. (b) The soft feedback symbols are computed from APPs.

the additional information provided by the current symbol. We emphasize that this performance gain depends on the assumptions of a large system and optimized P-DFD filters assuming perfect feedback. Further simulations indicate that the gap between the “waterfall” regions shown in Figs. 6(a) and 6(b) diminishes when the system size is reduced, and when the filters are estimated from the received data [21]. (Furthermore, extrinsic feedback can slightly outperform APP feedback.) Finally, comparing Fig. 6(b) with Fig. 2, for the particular code and parameters chosen, iterative soft decision feedback with APPs offers a gain of nearly 5 dB relative to hard decision feedback.

Because of the improved large-system performance of APP feedback relative to extrinsic feedback, and the accuracy of the large-system analysis, as shown in Fig. 6(b), in what follows we restrict our attention to APP feedback. Fig. 7 shows large-system error rate versus normalized user index \bar{k} for the IS-DFD

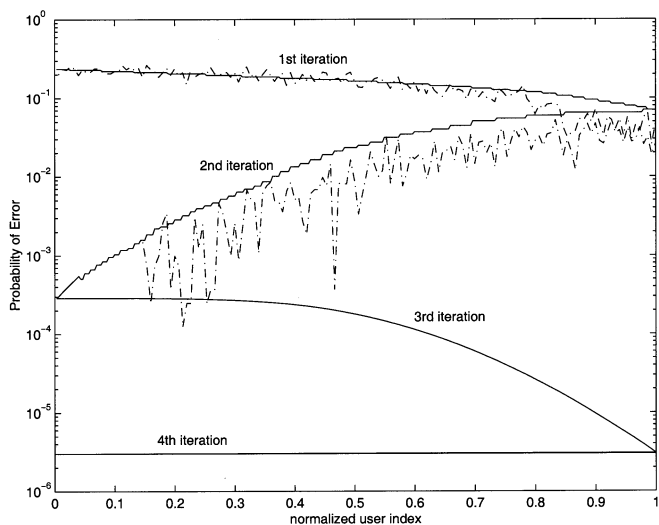


Fig. 7. Large-system error rate versus normalized user index for the IS-DFD. Simulated results with $K = 150$ are also shown.

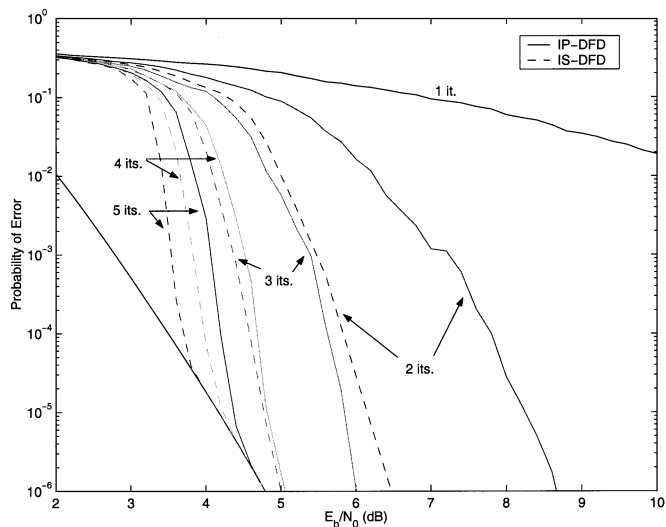


Fig. 8. Large-system error rate versus E_b/N_0 for IP- and IS-DFDs.

with APP feedback. The indexes $\bar{k} = 0$ and $\bar{k} = 1$ refer to the user decoded first and last, respectively, in the first iteration. The spectral efficiency $K/N = 0.75$ and $E_b/N_0 = 4.5$ dB. Also shown are the corresponding simulated results for $K = 150$. A fixed number of runs was used to generate the simulated results, so that the variance increases as the error rate decreases. The error rates for all users converge to the single-user bound with fewer iterations than those required by the IP-DFD.

Fig. 8 compares large-system error rates versus E_b/N_0 for the IP- and IS-DFDs. The parameters are the same as those used to generate Fig. 6. The IS-DFD curves for iterations 1–4 correspond to $\bar{k} = 0, 1, 0, 1$, respectively. The first iteration, therefore, corresponds to linear MMSE performance, and coincides with the P-DFD. These results show that the number of iterations required by the IS-DFD for convergence (for any user) is less than that required by the IP-DFD. Still, both the IS- and IP-DFDs converge to the same error rates given sufficient iterations.

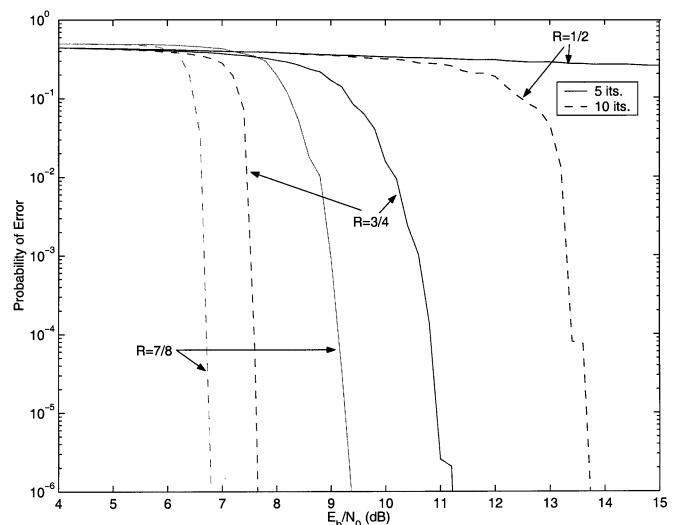


Fig. 9. Large-system error rate versus E_b/N_0 for different code rates with $K/N = 1.25$.

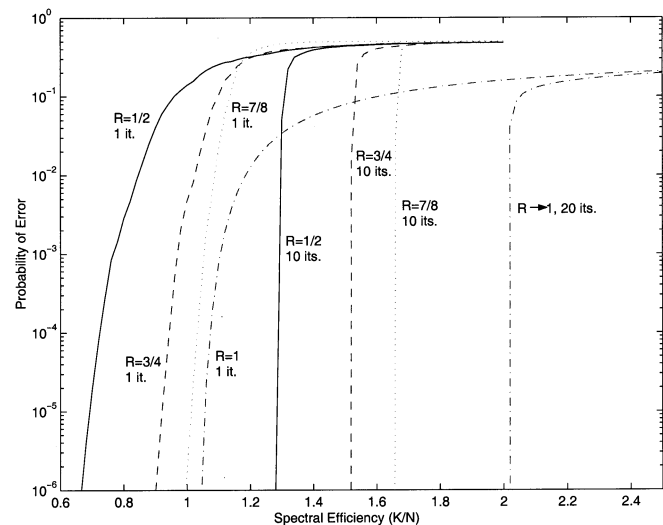


Fig. 10. Large-system error rate versus spectral efficiency with large E_b/N_0 .

B. Effect of Code Rate

Fig. 9 shows large-system error rate versus E_b/N_0 for the IP-DFD with spectral efficiency $K/N = 1.25$ and code rates $R = 1/2, 3/4$, and $7/8$. Curves are shown for five and ten iterations. For the relatively high spectral efficiency considered, the higher code rates give substantial performance improvements relative to the rate $1/2$ code. Fig. 10 shows large-system error rate versus spectral efficiency K/N with very large E_b/N_0 (100 dB) for different code rates. Curves corresponding to one and ten iterations are shown with coding. The curve for $R \rightarrow 1$ again assumes that $R \rightarrow 1$ from below with perfect interleaving. In that case, 20 iterations are needed for convergence. These plots demonstrate that the iterative receivers considered are interference limited. That is, for a given code, the maximum load \bar{K} that can be supported is finite even in the absence of noise. This maximum load is shown to increase with code rate, and tends to the load $\bar{K} \approx 2.01$ as the code rate $R \rightarrow 1$. In contrast, it has

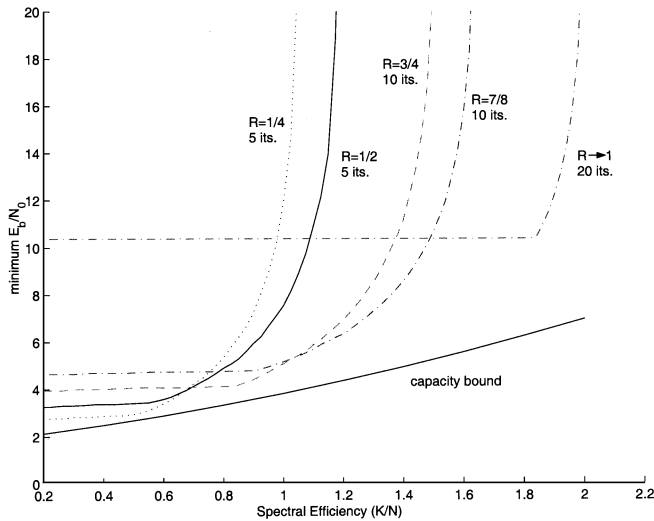


Fig. 11. Minimum E_b/N_0 required to achieve either the single-user bound, or an error rate of 10^{-6} with different code rates. The minimum E_b/N_0 corresponding to large-system capacity is also shown.

been shown in [22] that the optimal (ML) receiver is not interference limited.

Fig. 11 shows the minimum E_b/N_0 required by the IP-DFD to achieve either the single-user bound or an error rate of 10^{-6} (whichever is larger) as a function of spectral efficiency K/N . Curves are shown for code rates 1/4 and 1/2 with five iterations, code rates 3/4 and 7/8 with ten iterations, and $R \rightarrow 1$ with 20 iterations. The choice of iterations is based on the observation that more iterations are needed for convergence at higher loads. Also shown is the lower bound on minimum E_b/N_0 based on the large-system sum capacity with random spreading [9]. Letting $C(E_b/N_0; \rho)$ denote this large-system capacity as a function of E_b/N_0 and $\rho = K/N$ in bits per chip, the latter curve is the E_b/N_0 which satisfies $C(E_b/N_0; \rho) = \rho$, where ρ is the target spectral efficiency. This corresponds to binary signaling. These results show that the iterative receivers perform quite close to the capacity bound for spectral efficiencies $K/N < 0.9$, but diverge from the capacity bound as the K/N increases. As expected, low-rate codes perform better than high-rate codes at low spectral efficiencies, and the reverse is true at high spectral efficiencies.

VII. CONCLUSIONS AND EXTENSIONS

Large-system performance of iterative DFDs with parallel and successive demodulation has been studied. Soft decision feedback gives a substantial improvement in performance relative to hard decision feedback (e.g., nearly 5 dB with $K/N = 3/4$). In addition, our results show that APP feedback gives a substantial performance improvement relative to extrinsic feedback. With APP feedback at moderate spectral efficiencies, the soft iterative DFDs can achieve near-single-user performance at E_b/N_0 's close to the capacity limit. However, the iterative receivers are interference limited, in the sense that there is a maximum load \bar{K} that can be supported even in the absence of noise. For a large system, this maximum load increases with code rate to a value slightly greater than two as $R \rightarrow 1$.

Our results also show that with limited iterations, the IS-DFD can perform significantly better than the IP-DFD, although with sufficient iterations, both perform the same for the cases considered. Examples with coded hard decision feedback show that the IP-DFD requires only one or two additional iterations for convergence.

The analysis presented here can be extended to account for unequal received powers, asynchronous users, and multipath. Unequal received powers can be taken into account by using the formula for large-system SINR for the linear MMSE receiver with an arbitrary received power distribution presented in [8]. The analysis then proceeds as before, where the variance of the feedback error term must include an average over the power distribution of the cancelled users. For the S- and IS-DFD, this term depends on the user and the order in which the users are cancelled.

The extension to asynchronous CDMA is more difficult, but can be accomplished using techniques developed for the linear receiver in [23] and [18]. The feedback error terms must, of course, be averaged over the random delays. The effect of multipath can be taken into account for a particular user by conditioning on the user's channel, as in [24]. With small delay spreads (i.e., ignoring the intersymbol interference), the variance of the large-system multiple-access interference can be estimated as in [24] and [25].

Finally, we remark that the CDMA model analyzed here is equivalent to a single-user flat fading channel with multiple transmit and receiver antennas (e.g., see [26]). If the channel coefficients are i.i.d., then the large-system analysis presented here can be applied directly to a multiple-antenna system where the CDMA parameters K and N' become the number of transmit and receiver antennas, respectively.

APPENDIX

DERIVATION OF (16)–(18)

It is sufficient to derive these relationships for $\mathbf{R}_{U_k} = \mathbf{R}$. The first relation (16) follows directly from (11) and the matrix inversion lemma. To derive (17), we again apply the matrix inversion lemma

$$\begin{aligned} \mathbf{p}_k^\dagger \mathbf{R}^{-2} \mathbf{p}_k &= \mathbf{p}_k^\dagger \mathbf{R}_{k-}^{-2} \mathbf{p}_k \\ &\times \left[1 - \frac{2\mathbf{p}_k^\dagger \mathbf{R}_{k-}^{-1} \mathbf{p}_k}{1 + \mathbf{p}_k^\dagger \mathbf{R}_{k-}^{-1} \mathbf{p}_k} + \frac{(\mathbf{p}_k^\dagger \mathbf{R}_{k-}^{-1} \mathbf{p}_k)^2}{(1 + \mathbf{p}_k^\dagger \mathbf{R}_{k-}^{-1} \mathbf{p}_k)^2} \right] \\ &= \frac{\mathbf{p}_k^\dagger \mathbf{R}_{k-}^{-2} \mathbf{p}_k}{(1 + \mathbf{p}_k^\dagger \mathbf{R}_{k-}^{-1} \mathbf{p}_k)^2} \end{aligned} \quad (36)$$

where $\mathbf{R}_{k-} = \mathbf{R} - \mathbf{p}_k \mathbf{p}_k^\dagger$ is the interference-plus-noise covariance matrix. Now $\mathbf{p}_k^\dagger \mathbf{R}_{k-}^{-1} \mathbf{p}_k \rightarrow \beta_{\text{LIN}}$ and

$$\mathbf{p}_k^\dagger \mathbf{R}_{k-}^{-2} \mathbf{p}_k = -\frac{\partial}{\partial(\sigma^2)} (\mathbf{p}_k^\dagger \mathbf{R}_{k-}^{-1} \mathbf{p}_k) \quad (37)$$

$$\rightarrow -\frac{\partial \beta_{\text{LIN}}}{\partial(\sigma^2)} \quad (38)$$

in probability as $K \rightarrow \infty$. Computing the derivative and combining with (36) gives (17).

The multiple-access interference term (18) can be obtained by observing that the large-system SINR for the linear MMSE receiver is

$$\beta_{\text{LIN}}(\bar{k}) = \frac{[\kappa^*(\bar{k})]^2}{\psi^*(\bar{k}) + \sigma^2\gamma^*(\bar{k})}. \quad (39)$$

Solving for ψ^* and combining with (16) and (17) gives (18).

REFERENCES

- [1] P. D. Alexander, A. J. Grant, and M. C. Reed, "Iterative detection in code-division multiple-access with error control coding," *Eur. Trans. Telecommun.*, vol. 9, no. 5, pp. 419–425, Sept.–Oct. 1998.
- [2] M. C. Reed, C. B. Schlegel, P. D. Alexander, and J. A. Asenstorfer, "Iterative multiuser detection for CDMA with FEC: near-single-user performance," *IEEE Trans. Commun.*, vol. 46, pp. 1693–1699, Dec. 1998.
- [3] P. D. Alexander, M. C. Reed, J. Asenstorfer, and C. B. Schlegel, "Iterative multiuser interference reduction: turbo CDMA," *IEEE Trans. Commun.*, vol. 47, pp. 1008–1014, July 1999.
- [4] X. Wang and H. V. Poor, "Iterative (turbo) soft interference cancellation and decoding for coded CDMA," *IEEE Trans. Commun.*, vol. 47, pp. 1046–1061, July 1999.
- [5] H. El Gamal and E. Gerontotis, "Iterative multiuser detection for coded CDMA signals in AWGN and fading channels," *IEEE J. Select. Areas Commun.*, vol. 18, pp. 30–41, Jan. 2000.
- [6] G. Woodward and M. L. Honig, "Performance of adaptive iterative multiuser parallel decision feedback with different code rates," in *Proc. Int. Conf. Communications*, Helsinki, Finland, June 2001, pp. 852–856.
- [7] A. J. Grant and P. D. Alexander, "Random sequence multisets for synchronous code-division multiple-access channels," *IEEE Trans. Inform. Theory*, vol. 44, pp. 2832–2836, Nov. 1998.
- [8] D. N. C. Tse and S. V. Hanly, "Linear multiuser receivers: effective interference, effective bandwidth and user capacity," *IEEE Trans. Inform. Theory*, vol. 45, pp. 641–657, Mar. 1999.
- [9] S. Verdú and S. Shamai, "Spectral efficiency of CDMA with random spreading," *IEEE Trans. Inform. Theory*, vol. 45, pp. 622–640, Mar. 1999.
- [10] E. Biglieri, G. Caire, and G. Taricco, "CDMA system design through asymptotic analysis," *IEEE Trans. Commun.*, vol. 48, pp. 1882–1896, Nov. 2000.
- [11] W. Xiao and M. L. Honig, "Forward link performance of satellite CDMA with linear interference suppression and one-step power control," *IEEE Trans. Wireless Commun.*, vol. 1, pp. 600–610, Oct. 2002.
- [12] R. Müller, "Multiuser receivers for randomly spread signals: fundamental limits with and without decision-feedback," *IEEE Trans. Inform. Theory*, vol. 47, pp. 268–283, Jan. 2001.
- [13] P. Rapajic, M. L. Honig, and G. Woodward, "Multiuser decision feedback detection: Performance bounds and adaptive algorithms," in *Proc. Int. Symp. Information Theory*, Cambridge, MA, Aug. 1998, p. 34.
- [14] S. ten Brink, "Convergence behavior of iteratively decoded parallel concatenated codes," *IEEE Trans. Commun.*, vol. 49, pp. 1727–1737, Oct. 2001.
- [15] J. Boutros and G. Caire, "Iterative multiuser joint decoding: unified framework and asymptotic analysis," *IEEE Trans. Inform. Theory*, vol. 48, pp. 1772–1793, July 2002.
- [16] G. Woodward, R. Ratasuk, M. L. Honig, and P. Rapajic, "Multistage decision-feedback detection for DS-SS-CDMA," in *Proc. Int. Conf. Communications (ICC)*, Vancouver, BC, Canada, June 1999, pp. 68–72.
- [17] G. Woodward, R. Ratasuk, M. L. Honig, and P. B. Rapajic, "Minimum mean-squared error multiuser decision feedback detection for DS-SS-CDMA," *IEEE Trans. Commun.*, vol. 50, pp. 2104–2112, Dec. 2002.
- [18] J. Zhang, E. K. P. Chong, and D. N. C. Tse, "Output MAI distributions of linear MMSE multiuser receivers in DS-SS-CDMA systems," *IEEE Trans. Inform. Theory*, vol. 47, pp. 1128–1144, Mar. 2001.

- [19] I. E. Bocharova and B. D. Kudryashov, "Rational rate punctured convolutional codes for soft-decision Viterbi decoding," *IEEE Trans. Inform. Theory*, vol. 43, pp. 1305–1313, July 1997.
- [20] H. El Gamal and A. R. Hammons, "Analyzing the turbo decoder using the Gaussian approximation," *IEEE Trans. Inform. Theory*, vol. 47, pp. 671–686, Feb. 2001.
- [21] M. L. Honig, G. Woodward, and Y. Sun, "Adaptive iterative multiuser decision feedback detection," *IEEE Trans. Wireless Commun.*, to be published.
- [22] D. Tse and S. Verdú, "Optimum asymptotic multiuser efficiency of randomly spread CDMA," *IEEE Trans. Inform. Theory*, vol. 46, pp. 2718–2722, Mar. 2000.
- [23] K. Tse and D. N. C. Tse, "Effective bandwidths and effective interference for linear multiuser receivers in asynchronous systems," *IEEE Trans. Inform. Theory*, vol. 45, pp. 1426–1447, July 2000.
- [24] W. G. Phoel and M. L. Honig, "Performance of coded DS-SS-CDMA with pilot-assisted channel estimation and linear interference suppression," *IEEE Trans. Commun.*, vol. 50, pp. 822–832, May 2002.
- [25] J. Evans and D. N. C. Tse, "Linear multiuser receivers for multipath fading channels," *IEEE Trans. Inform. Theory*, vol. 46, pp. 2059–2078, Sept. 2000.
- [26] A. Paulraj and C. B. Papadias, "Space-time processing for wireless communications," *IEEE Signal Processing Mag.*, vol. 14, pp. 49–83, Nov. 1997.



Michael L. Honig (S'80–M'81–SM'92–F'97) received the B.S. degree in electrical engineering from Stanford University in 1977, and the M.S. and Ph.D. degrees in electrical engineering from the University of California, Berkeley, in 1978 and 1981, respectively.

He subsequently joined Bell Laboratories in Holmdel, NJ, where he worked on local area networks and voiceband data transmission. In 1983 he joined the Systems Principles Research Division at Bellcore, where he worked on Digital Subscriber Lines and wireless communications. Since the Fall of 1994, he has been with Northwestern University, Evanston, IL, where he is a Professor in the Electrical and Computer Engineering Department. He was a visiting lecturer at Princeton University, Princeton, NJ, during the Fall of 1993, a visiting Mackay Professor at the University of California, Berkeley, for Fall 2000, and a visiting scholar at the University of Sydney, Sydney, Australia, during the summer of 2001. He has also worked as a freelance trombonist.

Dr. Honig has served as an editor for the IEEE TRANSACTIONS ON INFORMATION THEORY (1998–2000) and the IEEE TRANSACTIONS ON COMMUNICATIONS (1990–1995), and was a guest editor for the *European Transactions on Telecommunications and Wireless Personal Communications*. He has also served as a member of the Digital Signal Processing Technical Committee for the IEEE Signal Processing Society, and as a member of the Board of Governors for the Information Theory Society for 1997–2003. He is the corecipient of the 2002 IEEE Communications Society and Information Theory Society Joint Paper Award.



Rapeepat Ratasuk (S'95–M'02) received the B.S., M.S., and Ph.D. degrees in electrical engineering from Northwestern University, Evanston, IL, in 1994, 1996, and 2000, respectively.

Since 1999, he has been with Motorola, Inc., Arlington Heights, IL, as a Systems Engineer in the Network Advanced Technologies Group. His current research interests are in the design and performance of next-generation wireless communication systems.